RETROSPECTIVE STUDY OF VERTICAL GROUND DEFORMATION IN COMO, NORTHERN ITALY: INTEGRATION OF LEVELLING AND PSI MEASUREMENTS

R. Eskandari [1] *, M. Scaioni [1]

[1] Dept. of Architecture, Built Environment and Construction Engineering, Politecnico di Milano, via Ponzio 31, 20133 Milano, Italy
rasoul.eskandari@mail.polimi.it, marco.scaioni@polimi.it

KEY WORDS: Deformation, ERS, Levelling, PSInSAR, Synthetic Aperture Radar, Subsidence, Validation

ABSTRACT:

Subsidence-related vertical ground deformation due to natural and anthropogenic factors may lead to considerable damages to structures and infrastructures, and may increase the occurrence probability of consequential events, such as floods, especially on sea and lake shores. Como city, placed in the north of Italy, adjacent to Como Lake, is subjected to significant subsidence phenomenon, which has been monitored by geodetic levelling networks. In this work the historical geodetic levelling measurements and satellite-based Synthetic Aperture Radar (SAR) data archive are integrated to assess the accuracy of Atmospheric Delay and Deformation Rate estimations obtained through Persistent Scatter Interferometry (PSI) techniques. Tree levelling measurement datasets acquired in 1990, 1997 and 2004 are used in order to obtain the precise deformation rate at the benchmarks for two periods of 1990-1997 and 1997-2004. For multi-temporal InSAR analysis, 106 SAR images (1992-2004) and 41 SAR images (1992-2004) in Ascending Track orbit from ERS-1/2 missions are used in this study. The assessment is performed through a statistical comparison between two sets of vertical land deformation rates obtained by integrated methods. The results of the validation represented a good consistency between deformation rates derived by both techniques. Also, this study has revealed the potential of SAR images acquired in gyro-less mode by ERS-2 mission (2001-2004) in terms of the estimation of ground deformation.

1. INTRODUCTION

Ground surface is subjected to progressive vertical displacements, due to subsidence, volcanic and tectonic activities, earthquakes, landslides, etc. Among these, subsidence is commonly defined as sudden sinking or graduate lowering of the ground surface (Galloway and Burbey, 2011). In general, the principal causes may be categorized into natural (e.g., natural consolidation, dissolution of carbonate rocks, and organic matter oxidation, isostatic adjustment), anthropogenic (e.g., fluid withdrawal, and underground tunnelling and mining), and the interacted effect of both groups (Galloway et al., 1999; Carminati et al., 2003).

As a catastrophic event, the sudden type of subsidence such as sinkholes may cause human losses (Tomás et al., 2014). On the other hand, the gradual deformations in terms of subsidence, through which the formation of casualties is rare, may cause: i) occurrence of differential displacements at the foundation of buildings and infrastructures (Solari et al., 2018) bringing instability problems and increasing collapse possibility, and ii) severe cumulative lowering of the ground surface amplifying the probability of permanent inundation and flooding (Nappo et al., 2020), especially in sea and lake shores. These may lead to significant damages and economic losses (Wu et al., 2009), and amplification of subsidence-related hazards (Mohamadi et al., 2019).

Como town, placed in the north of Italy as shown in Figure 1(a), is the case study of this work. The town lies on a sedimentary basin with the presence of unconsolidated silty sediments. Being located at the end of the western branch of the Lake of Como, the basin is formed by sediments collected from a large drainage plain of 45,000 km^2 which is drained by Cosia and Valduce water courses (Ferrario et al., 2015). Based on the proposed hydro-geotechnical model (Bajni et al., 2019) and several similar works devoted to Como basin, the poor mechanical properties of the basin beneath the historic area of the town, as the main natural factor, may subject the area to serious hazards such as subsidence and flooding. A simplified geological map of the Como basin is provided in Figure 1(b), and the legend description is summarized in Table 1. For a complete description on the stratigraphic architecture of the basin, refer to Ferrario et al. (2015) and Nappo et al. (2020).

The major anthropogenic factors modifying the natural trend of land lowering during the past 70 years of Como town have been diagnosed, and their effects on the subsidence rate variations have been studied by several works. They include excessive water extraction from wells penetrating deep aquifers, overburden stress caused by urban development, buildings and anti-flooding facilities construction, and road traffic (see Comune di Como, 1980; Comerci et al., 2007; Nappo et al., 2021).

Traditional geodetic measurements, such as optical levelling operations (e.g., Trahan, 1982; Fabris et al., 2014)) and Global Navigation Satellite Systems (GNSS) (e.g., Jing-Xiang and Hong, 2009; Ustun et al., 2010), may provide precise and reliable observations for measuring ground deformations. These techniques are characterized by key limitations, for example: limited number of benchmarks to be measured, expensive operations in terms of equipment and experts in the field, time-consuming on-site activities, and practically slow repeating time (Psimoulis et al., 2007; Macchiarulo et al., 2021).

Besides these practical challenges, and temporal and spatial limitations, the atmospheric issues and temperature differences (due to the relatively long period of levelling operations, for example) affecting the measurements in the acquisition phase are another problem that may not be easily tackled.

* Corresponding author

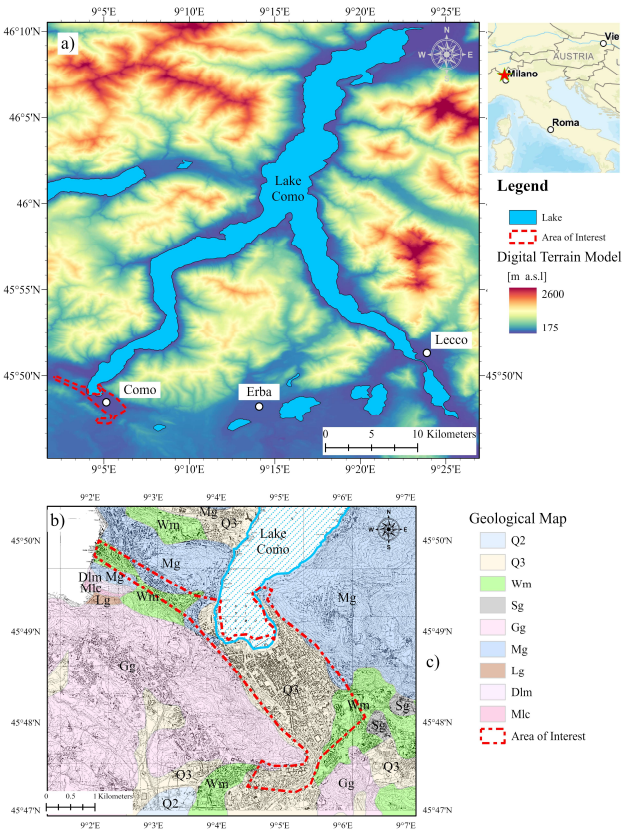

Figure 1. Case study of Como town: a) geographic location in Italy and with respect to the Lake of Como shown on a Digital Terrain Model (DTM) (Heli-Dem HD2 for Western Alpine - Biagi et al., 2016), and b) simplified geological map shown on a regional technical map (Carta Tecnica Regionale: CTR - Regione Lombardia, 2022) with a scale of 1:10,000 (reference system: WGS 84/UTM Zone 32).

In last decades, *Synthetic Aperture Radar Interferometry* (InSAR) has been known as promising and relatively low-cost alternative for multiscale monitoring of vertical displacements (Yang et al., 2022) thanks to approximately global coverage and high-revisit frequency (Nilfouroushan et al., 2022). Taking advantage of extensive amount of SAR data archives, *Persistent Scatterer Interferometry* (PSI) enables reliable estimation of ground-deformation time history and topographic information. These techniques, started by a pioneering work by Ferretti et al. (2001) proposing Permanent Scatterer InSAR (PSInSAR™), benefits from the specific characteristics of coherent and sensor-friendly targets on the ground. This work has been followed by several other techniques and proposed algorithms by the aim of overcoming different sources of decorrelations and limitations. Some of the commonly used techniques are Small Baseline Subset (SBAS - Berardino et al., 2002), Interferometric Point Target Analysis (IPTA - Werner et al., 2003), Delft Persistent Scatterer Interferometry (DePSI - Kampes, 2005), Persistent Scatterer Pairs (PSP - Costantini et al., 2008) among others.

Thanks to the reliable extraction of useful information about the ground surface and corresponding changes, these techniques have been widely exploited for monitoring and measuring the ground variations, using several sensors from ERS (low resolution) to Cosmo-SkyMed (CSK) (high resolution), at different scales spanning from single buildings up to the national scale.

Type	Description	Geological Period	Lithology
Q2	Alluvial Fan	Late Glacial and Lacustrine Holocene	Clays and Silts
Q3	Fluvio-glacial and Fluvial Wurm	Late Pleistocene	Gravels and Sands
Wm	Moraine Wurm	Late Pleistocene	Gravels, Silts, and Blocks
Sg	Sandstone Group	Late Cretaceous (Santonian – Turonian)	Sandstones
Gg	Gonfolite Group	Early Miocene (Burdigalian-Oligocene)	Conglomerates, Sandstones, and Marls
Mg	Medolo Group (Red Ammonite)	Early Jurassic (Toarcian and Aalenian) to Hettangian	Marls, Marly and Flint Limestones
Lg	Limestone Group	Eocene to Paleocene	Nummulitic Limestone
Dlm	Dolomite (Conchodon type)	Early Jurassic to Rhaetian	Limestone and Dolomitic Limestone
Mlc	Maiolica	Late Jurassic (Barremain – Tithonian)	Marly and Flint Limestones, and Marls

Table 1. Description of geological map (Regione Lombardia, 2018).

Besides the land displacement monitoring all around the world (Cando Jácome et al., 2020; Cigna and Tapete, 2021; Fernández-Merodo et al., 2021; Mirzadeh et al., 2021; Modeste et al., 2021; Peng et al., 2022; Shi et al., 2022), *land subsidence* has been extensively monitored and evaluated in Italy, from south (Cianflone et al., 2015; 2018; Amato et al., 2020), center (Del Soldato et al., 2018; Bianchini et al., 2019; Ciampalini et al., 2019; Ezquerro et al., 2020), to north (Farolfi et al., 2019). This major focus is given arise by the fact that Italy is particularly known to be prone to natural subsidence experiencing significant accelerations due to human activities, especially in built-up environment, starting from the last century (Solari et al., 2018).

Integration of InSAR-derived deformation data with moderate to high-precision traditional *geodetic measurements*, such as GNSS (Farolfi et al., 2019a; 2019b; Xu et al., 2021) and optical leveling measurements (Amighpey and Arabi, 2016; Busetti et al., 2020; Yan et al., 2021), has been a powerful tool for correction and validation of different estimations through InSAR techniques. These estimations can be categorized as separate or combined action of deformation, height, seasonal, and atmospheric contribution (Li et al., 2005), which can be obtained through *Multi-Temporal Differential InSAR* (MT-DInSAR) discussed in Section 3. Also, the data acquired by different geodetic measurements (for example InSAR techniques for short-wavelength and GNSS for long-wavelength deformation velocity models (Shen and Liu, 2020)) can be combined through data fusion approaches to generate more consistent and accurate information on the study area.

In this work, the historical geodetic levelling measurements and satellite-based SAR data archive covering Como town are integrated to assess the accuracy of Atmospheric Delay and Deformation Rate estimations obtained through PSI techniques implemented in SAPROZ® software package (Perissin et al., 2011). The assessment is performed through a comparison between two sets of vertical land deformation rates obtained by integrated methods.
This is the first time that historic data acquired on Como levelling network are integrated to another measurement technique. Since the extraction of the InSAR-derived vertical ground displacements in the period 1997-2004 is performed using ERS-2 SAR images, which are acquired in gyro-less piloting mode (Miranda et al., 2005), this study shows the potential of these type of SAR images for InSAR purposes.

2. GEODETIC LEVELLING MEASUREMENTS

Although the *geodetic levelling* operations have been carried out once in a few years starting from 1879 by IGMI (official Italian authority for mapping and surveying) and stopped in 2004, no useful data are available until 1995 to study the land subsidence in the town due to the change of benchmarks between measurement campaigns (Colombo et al., 1998). The numerical data of measurements have been extracted directly from the repository of the former Surveying Department of Politecnico di Milano, such as tabular data concerning levelling campaigns of 1997 and 2004 (Bonci et al., 2004). The geo-positiong and digitalization of the data points have been performed based on the database and documentation provided by IGMI (1990).
From 1955 to 2004, three last measurement datasets acquired in 1990, 1997 and 2004 have been used to obtain the precise deformation rate at the benchmarks within the levelling network. The deformation rate at each benchmark have been derived by dividing the difference between two height measurements by the temporal baseline of the measurements. Figures 2 and 3 show the annual vertical ground deformation rate R_d (in mm/year) for the periods 1990-1997 and 1997-2004, respectively. For the first period, only 62 benchmarks were available to represent the deformation rate. However, this number is 85 for the second period. In both cases, the rates between +0.50 and -0.50 mm/year are considered to be neutral vertical land displacement and are shown in green colours in Figures 2 and 3. It should be mentioned that the reference point for all the levelling operations is the left-most point in the southern tail of the study area, placed in Camerlata suburb of Como town.
In the period of 1990-1997, the most study area was roughly subjected to a neutral vertical land change, with a slight uplift at the southern portion of the town, and a moderate subsidence very close to the lakefront, especially on Caldirola breakwater (in Italian: “diga foranea”) located at the north of downtown.
In the case of the 1997-2004 differences, the most severe subsidence of 11.30 mm/year could be seen near the “Tempio Voltiano” building at the lakefront located at the north of downtown. The breakwater and the zone connecting this to the downtown area are subjected to moderate land lowering and most of this area is subjected to slight subsidence. The interesting behaviour of the rates can be seen in the foothill of the mountains located at NE and SW of the study area with, respectively, uplift in the interval +1.00 to 3.27 mm/year and subsidence in the interval -3.00 to -5.50 mm/year, which is in contrast with the previous period.

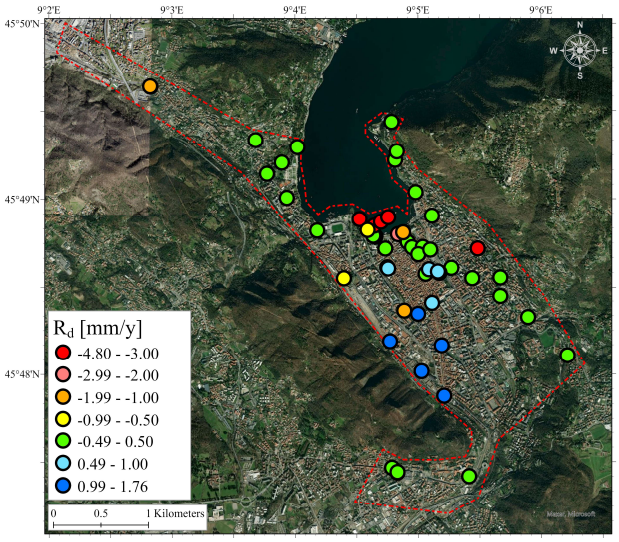

Figure 2. vertical ground deformation rate R_d (in mm/year) for the period of 1990-1997 at 62 available levelling benchmarks.

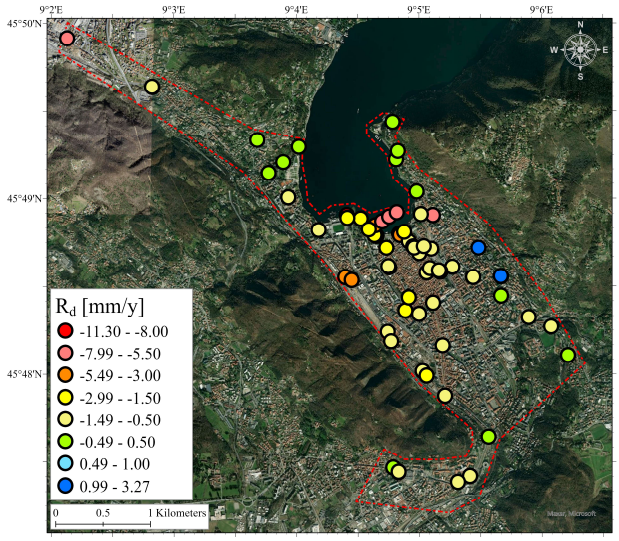

Figure 3. vertical ground deformation rate R_d (in mm/year) for the period of 1997-2004 at 85 available levelling benchmarks.

3. MULTI-TEMPORAL INSAR ANALYSIS

3.1 Methodology and Data Collection

In this work, all the required steps, from importing and co-registration of SAR images to the estimation of ground deformations have been done in SARPROZ© software package (Perissin et al., 2011). This powerful InSAR processing tool implemented in MATLAB, provides a flexible environment for the user to have full control of any technical aspect of PSI analysis. The software was successfully used by several research groups for linear and non-linear deformation monitoring in different applications, such as land subsidence (Fryksten and Nilfouroushan, 2019; Cando Jácome et al., 2020), infrastructures (Bakon et al., 2014; Lyu et al., 2020), and dams (Ruiz-Armenteros et al., 2021) among others.
Considering the very basic DInSAR equation and its components (González and Fernandez, 2011), the flat and height components are easily removed by means of imported

external data (orbital data and Digital Elevation Model - DEM). In this work, ERS Precise Orbital Data (POD) provided by the European Space Agency (ESA), and DTM Heli-DEM HD2 (Biagi et al., 2016) have been used for these purposes.
The software takes advantage of high number of SAR images in the context of Multi-Temporal Differential InSAR (MT-DInSAR) to estimate the Atmospheric Delay (one of the key challenges in InSAR processing). For this purpose, a unique technique based on PSP algorithm (Costantini et al., 2008) is used, which requires choosing a proper initial set of Persistent Scatterer (PS) candidates.
Then, the combined effect of Deformation, Residual Heigh, and Temperature in the context of DInSAR are estimated per each PS candidates using the standard technique of PSInSAR. It should be mentioned that the graph connection (how the SAR images are going to be paired for interferometric analysis) used for all the PS processing operations is "Star" graph in this study. The properties and the number of ERS SAR images used in this study are summarized in Table 2.

Spectral Band	**C-Band**	
Acquisition Mode and Spatial Resolution	IMS Medium-Resolution (~30m)	
Signal Wavelength and Frequency	5.66 cm 5.3 GHz	
Nominal Revisit Time	35 days	
Orbit Track	Descending	Ascending
Observation Period	30 April 1992 11 April 2004	04 June 1992 11 April 2004
Number of Images	106	41
Looking Angle	23.22 °	23.29 °

Table 2. Properties of ERS-1/2 SAR (Synthetic Aperture Radar) images.

3.2 Period 1992-1997: Descending Track

43 ERS SAR images acquired in Descending Track in the period 1992-2004 have been imported, and after cropping the area of interest and co-registration, the preliminary tasks for initial SAR image processing have been performed to obtain Amplitude Stability Index (AmpStabI) and Spatial Coherence (γ_{Sp}) for identifying coherent pixels in terms of both amplitude and phase.
Then, by choosing the pixels having values of:

$$(\text{AmpStabI}+\gamma_{Sp}) \geq 1.1 \quad (1)$$

as PS candidates, the Atmospheric Phase Screen (APS) for each interferometric pair has been produced (assuming a linear deformation trend between the PS pairs, presence of residual height and seasonal effect, and a "Flowered tree" network of connections among PS candidates). After removal of the known components, different useful information has been obtained by applying Multi-Temporal PS processing for each PS chosen, including: i) Line of Sight (LOS) Deformation trend (if linearity is assumed) and time histories; ii) Residual Height; iii) Thermal Expansion Coefficient; and iv) Temporal Coherence (γ_{Tm}).
It is obvious that estimations in all the chosen PS candidates are not satisfying, and it is identifiable by the value of γ_{Tm} per each PS. Here, the PSs with the values of $\gamma_{Tm} \geq 0.53$ are chosen as the final data points. Then, the LOS deformation rates has been transferred into vertical displacement velocity by being divided by cosine of look angle (provided in Table 2), assuming that the vertical component is the dominant one. The spatial distribution of vertical velocities over the study area is shown in Figure 4.

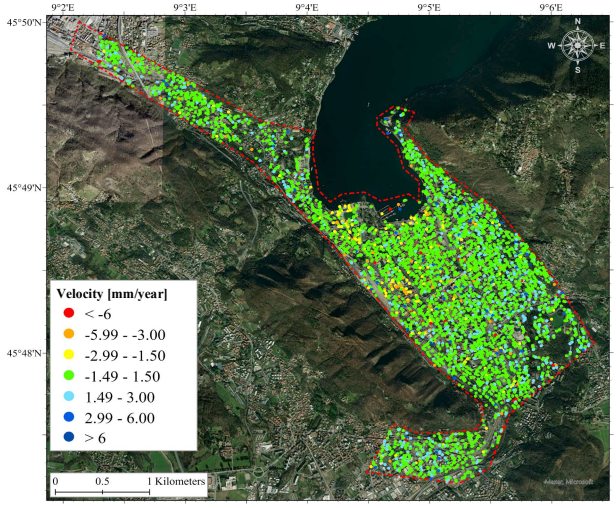

Figure 4. InSAR-derived vertical displacement velocity related to period 1992-1997 using ERS SAR images in Descending Track.

3.3 Period 1997-2004: Descending Track

The challenge concerning the SAR images in the period of 2001 to 2004, is the high values of Doppler Centroid (DC) differences. It has been observed that the InSAR processing using all 64 SAR images in the whole temporal interval suffers from values of DC even higher than 1. Therefore, in this study, this value has been limited to 0.5, which has resulted in the removal of 14 images belonging to the pilot period of gyro-less mode. The same procedure for APS estimation and Multi-Temporal PS processing (see Subsect. 3.2) has been used, considering that a non-linear deformation has been considered for the connections established among PS candidates for APS estimation. These solutions have been the most effective approaches, among several analyses with different parameters, to obtain a relatively regular spatial distribution of vertical displacement velocities over the area of interest (see Fig. 5).

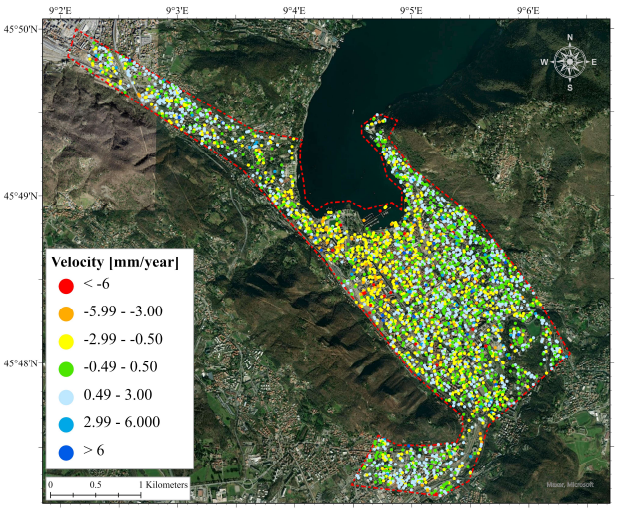

Figure 5. InSAR-derived vertical displacement velocity related to period 1997-2204 using SAR images in Descending Track.

3.4 Ascending Track

The SAR images acquired in this track have been diagnosed by a technical problem in terms of amplitude and phase components, especially in the period 1992-1997. The discussion about these issues is out of the scope of this study. Considering that the small number of images used in each period has not been sufficient to obtain reliable results in terms of ground deformations, and due to the problem mentioned above, these data have not used to achieve the purpose of this study.

4. VALIDATION

In this assessment, the biggest challenge has been the low resolution of the ERS SAR images, and the relatively high level of sparseness associated with the points containing the derived information. Also, the geocoding of the InSAR data points (PSs) may be done with several errors due to the inevitable inaccuracies present in orbital satellite data and the external DEM. Consequently, this may affect the real location of estimated points in the interpolation phase. To overcome these issues, a circle (hereafter called "buffer") has been defined around each levelling benchmark as the point containing valid information. Those target dataset's points falling within this buffer (called "buffer points") have been considered for the validation process. These buffers, which are constant throughout the validation procedure, are characterized by a center located at levelling benchmarks with a radius of approx. 35 m.

Considering the value of vertical deformation velocity per each levelling benchmark and the N points within the corresponding buffer, two well-known statistical parameters (Yang et al. 2022) have been adopted for the evaluation of difference between both datasets: i) *Absolute Error* (AE): which is calculated as the difference between "velocity at the levelling benchmark V_{LB}" and "mean velocity of the InSAR points in the corresponding buffer V_{InSAR}", and ii) *Root Mean Square Error* (RMSE). These quantities are shown in terms of histogram and fitted Log-normal Probability Density Function (LognPDF), and empirical Cumulative Distribution Function (ECDF), for both periods under investigation. The results are shown in Figures 7 and 8 for both periods 1992-1997 and 1997-2004. The mean number of PSs falling into the buffers around the levelling benchmarks are also provided in these figures per each period.

In general, the period 1992-1997 has resulted in better results in terms of the maximum error obtained and LognPDF parameters, w.r.t. the last period. This may be due to the problems regarding the gyro-less acquisition of SAR images after 2001, which shows the importance of DC differences in the accuracy of the estimations.

Approximately, Figure 6 shows a dense concertation of AEs distribution in the interval of 0 to 2 mm/year, and in terms of RMSE distribution in the interval from 0 to 3 mm/year. This dense concentration of the AE and RMSE for the last period is 0 to 4 mm/year and 0 to 5 mm/year, respectively, which is shown in Figure 7.

The very few exceedances from these reasonable intervals can be related to the local errors arisen from APS estimation and temporal decorrelations in InSAR processing. However, the density of distributions in these intervals shows the acceptable reliability and accuracy of the combined effect of APS estimation and Multi-Temporal PS processing used in this work for both periods.

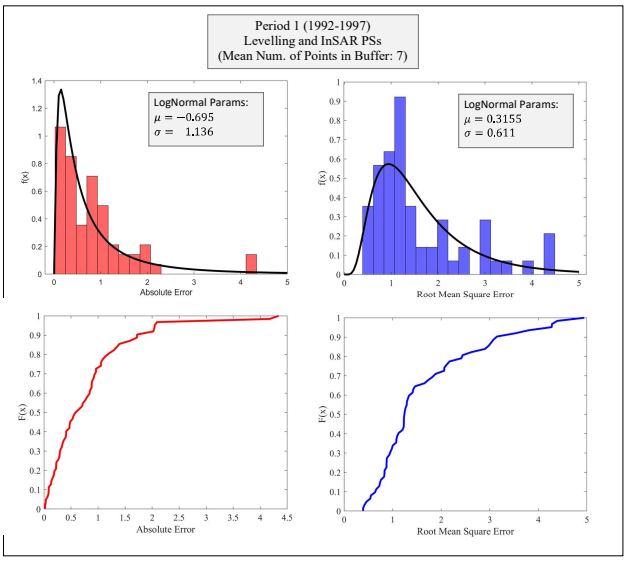

Figure 6. Statistical Assessment using *Absolute Error* (AE) and *Root Mean Square Error* (RMSE): optical levelling measurements and InSAR persistent scatterers (PSs) in the period 1992-1997.

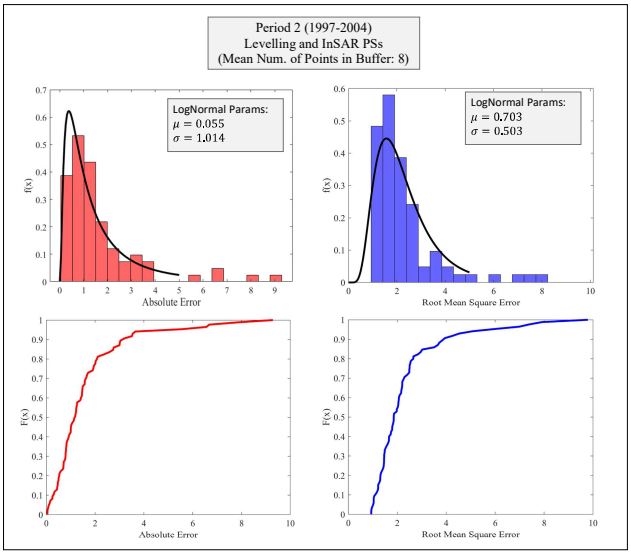

Figure 7. Statistical Assessment using AE and RMSE: optical levelling measurements and InSAR PSs in the period 1997-2004.

5. CONCLUSIONS

This work is devoted to the integration of optical levelling measurements and Persistent Scatterer Interferometry (PSI) techniques for retrospective evaluation of vertical ground deformations in Como town. The levelling-derived displacement rates have been compared to the displacement velocities obtained through Multi-Temporal PS InSAR processing using SARPROZ© software package, which has been performed by careful use of ERS SAR images due to the old data archive and different technical issues.

According to the Absolute Error parameter, the density of error distribution is approximately focused on the interval of values lower than 2 and 4 mm/year for the periods 1992-1997 and 1997-2004, respectively. These values are identified to be 3 and 5 mm/year based on Root Mean Square Error. Only a few

exceedances from these reliable values have been detected in some comparison points, which can be related to the inevitable local errors in data archive and corresponding processing.
These results show a reliable consistency between the compared techniques and, again, prove the high performance of PSInSAR analysis in terms of ground deformation estimation, as a powerful alternative monitoring technology. Also, it has been seen that the ERS SAR images acquired in gyro-less mode can be used for MT InSAR processing by limiting the values of Doppler Centroid differences and with the implementation of specific assumptions and considerations.
It should be noted that the results taken into consideration in this study are obtained through MT InSAR processing of ERS SAR images acquired in Descending Track, whilst the images acquired in Ascending Track are suggested to be ignored (for this area, in the period 1992-2004) due to serious technical issues and the small number of available data, which significantly affect the results.

ACKNOWLEDGEMENTS

The authors would like to thank Dr. Daniele Perissin for providing SARPROZ© tool for SAR and InSAR processing carried out in this work and Dr. Alfredo Rocca for the technical support. We would like also to acknowledge the European Space Agency for delivering ERS-1/2 data sets.

REFERENCES

Amato, V., Aucelli, P.P.C., Corrado, G., Di Paola, G., Matano, F., Pappone, G.,Schiattarella, M., 2020: Comparing geological and Persistent Scatterer Interferometry data of the Sele River coastal plain, southern Italy: Implications for recent subsidence trends. *Geomorph.* 351, paper no. 106953.

Amighpey, M.,Arabi, S., 2016: Studying land subsidence in Yazd province, Iran, by integration of InSAR and levelling measurements. *Remote Sensing Applications: Society and Environment* 4:1-8.

Bajni, G., Apuani, T., Beretta, G.P., 2019: Hydro-geotechnical modelling of subsidence in the Como urban area. *Eng. Geol.* 257, paper no. 105144.

Bakon, M., Perissin, D., Lazecky, M.,Papco, J., 2014: Infrastructure non-linear deformation monitoring via satellite radar interferometry. *Procedia Technology* 16: 294-300.

Berardino, P., Fornaro, G., Lanari, R.,Sansosti, E., 2002: A new algorithm for surface deformation monitoring based on small baseline differential SAR interferograms. *IEEE Trans.Geosci. Remote Sens.* 40(11): 2375-2383.

Biagi, L., Caldera, S., Carcano, L.,Negretti, M., 2016: The open data HELI-DEM DTM for the western alpine area: computation and publication. *Appl. Geom.* 8(3):191-200.

Bianchini, S., Solari, L., Del Soldato, M., Raspini, F., Montalti, R., Ciampalini, A., Casagli, N., 2019: Ground subsidence susceptibility (GSS) mapping in Grosseto Plain (Tuscany, Italy) based on satellite InSAR data using frequency ratio and fuzzy logic. *Remote Sens.* 11(17), paper No. 2015.

Bonci, L., Cametti, A., Comerci, V., Matarazzo, D., Michetti, A.M., Vittori, E.,Vullo, F., 2004. *Citta di Como - Livellazione di Alta Precisione - Anno 2004*: APAT (Agenzia per la Protezione dell'Ambiente e per i Servizi Tecnici), Rome (in Italian).

Busetti, A., Calligaris, C., Forte, E., Areggi, G., Mocnik, A.,Zini, L., 2020: Non-invasive methodological approach to detect and characterize high-risk sinkholes in urban cover evaporite karst: Integrated reflection seismics, PS-INSAR, leveling, 3D-GPR and ancillary data. a Ne Italian case study. *Remote Sens.* 12(22), paper No. 3814.

Cando Jácome, M., Martinez-Graña, A.M.,Valdés, V., 2020: Detection of terrain deformations using InSAR techniques in relation to results on terrain subsidence (Ciudad de Zaruma, Ecuador). *Remote Sens.* 12(10), paper No. 1598.

Carminati, E., Doglioni, C., Scrocca, D., 2003: Apennines subduction-related subsidence of Venice (Italy). *Geophys. Res. Lett.* 30(13), paper No. 1717.

Ciampalini, A., Solari, L., Giannecchini, R., Galanti, Y.,Moretti, S., 2019: Evaluation of subsidence induced by long-lasting buildings load using InSAR technique and geotechnical data: The case study of a Freight Terminal (Tuscany, Italy). *Int. J. Appl. Earth Obs. Geoinform.* 82, paper No. 101925.

Cianflone, G., Tolomei, C., Brunori, C.A.,Dominici, R., 2015: InSAR time series analysis of natural and anthropogenic coastal plain subsidence: The case of Sibari (Southern Italy). *Remote Sens.* 7(12):16004-16023.

Cianflone, G., Tolomei, C., Brunori, C.A., Monna, S.,Dominici, R., 2018: Landslides and subsidence assessment in the Crati Valley (Southern Italy) using InSAR data. *Geosci.* 8(2), paper No. 67.

Cigna, F.,Tapete, D., 2021: Satellite InSAR survey of structurally-controlled land subsidence due to groundwater exploitation in the Aguascalientes Valley, Mexico. *Remote Sens. Env.* 254, paper No. 112254.

Colombo, A., Giussani, A., Scaioni, M., Vassena, G., 1998: High Precision Leveling Network of Como Area for Subsidence Analysis. *Int. Arch. Photogramm. Remote Sens.*, Vol. 32, Part 6W4: 105-110.

Comerci, V., Capelletti, S., Michetti, A.M., Rossi, S., Serva, L.,Vittori, E., 2007: Land subsidence and Late Glacial environmental evolution of the Como urban area (Northern Italy). *Quatern. Int.* 173-174:67-86.

Comune di Como, 1980: *Relazione di sintesi della Commissione per lo Studio dei fenomeni di Subsidenza*. Documenti e Ricerche 34, Commissione Subsidenza, Comune di Como, Italy (in Italian).

Costantini, M., Falco, S., Malvarosa, F., Minati, F., 2008: A New Method for Identification and Analysis of Persistent Scatterers in Series of SAR Images. In: Proc. IEEE Int. Geoscience and Remote Sensing Symp. (IGARSS) 2008, Vol. 2, pp. 449-452.

Del Soldato, M., Farolfi, G., Rosi, A., Raspini, F.,Casagli, N., 2018: Subsidence evolution of the Firenze–Prato–Pistoia plain (Central Italy) combining PSI and GNSS data. *Remote Sens.* 10(7), paper No. 1146.

Ezquerro, P., Del Soldato, M., Solari, L., Tomás, R., Raspini, F., Ceccatelli, M., Fernández-Merodo, J.A., Casagli, N., Herrera, G., 2020: Vulnerability Assessment of Buildings due to Land Subsidence Using InSAR Data in the Ancient Historical City of Pistoia (Italy). *Sensors* 20(10), paper No. 2749.

Fabris, M., Achilli, V., Menin, A., 2014. Estimation of subsidence in Po Delta area (Northern Italy) by integration of GPS data, high-precision leveling and archival orthometric elevations. *Int. J. Geosci.* 5(06), paper No. 571.

Farolfi, G., Bianchini, S., Casagli, N., 2019a. Integration of GNSS and Satellite InSAR Data: Derivation of Fine-Scale Vertical Surface Motion Maps of Po Plain, Northern Apennines, and Southern Alps, Italy. *IEEE Trans. Geosci. Remote. Sens.* 57(1): 319-328.

Farolfi, G., Del Soldato, M., Bianchini, S., Casagli, N., 2019b. A procedure to use GNSS data to calibrate satellite PSI data for the study of subsidence: an example from the north-western Adriatic coast (Italy). *Europ. J. Remote Sens.* 52(sup4): 54-63.

Fernández-Merodo, J.A., Ezquerro, P., Manzanal, D., Béjar-Pizarro, M., Mateos, R.M., Guardiola-Albert, C., García-Davalillo, J.C., López-Vinielles, J., Sarro, R., Bru, G., 2021. Modeling historical subsidence due to groundwater withdrawal in the Alto Guadalentín aquifer-system (Spain). *Eng. Geol.* 283: paper No. 105998.

Ferrario, M.F., Bonadeo, L., Brunamonte, F., Livio, F., Martinelli, E., Michetti, A.M., Censi Neri, P., Chiessi, V., Comerci, V., Höbig, N., 2015. Late Quaternary environmental evolution of the Como urban area (Northern Italy): A multidisciplinary tool for risk management and urban planning. *Eng. Geol.* 193: 384-401.

Ferretti, A., Prati, C.,Rocca, F., 2001. Permanent scatterers in SAR interferometry. *IEEE Trans. Geosci. Remote. Sens.* 39(1): 8-20.

Fryksten, J.,Nilfouroushan, F., 2019. Analysis of clay-induced land subsidence in Uppsala City using Sentinel-1 SAR data and precise leveling. *Remote Sens.* 11(23), paper no. 2764.

Galloway, D.L.,Burbey, T.J., 2011. Review: Regional land subsidence accompanying groundwater extraction. *Hydrogeol. J.* 19(8): 1459-1486.

Galloway, D.L., Jones, D.R.,Ingebritsen, S.E., 1999. *Land subsidence in the United States*. U.S.G.S., The United States. doi.org/10.3133/cir1182.

González, P.J., Fernandez, J., 2011. Error estimation in multitemporal InSAR deformation time series, with application to Lanzarote, Canary Islands. *J. Geophys. Res. - Solid Earth* 116(B10), paper No. B10404.

IGMI, 1990. Documentazione Monografica dei Capisaldi Utilizzati per il Controllo dell Subsidenza nella Citta di Como. Direzione Geodetica (Istituto Geografico Militare Italiano), IGMI, Florence, Italy (in Italian).

Jing-Xiang, G., Hong, H., 2009. Advanced GNSS technology of mining deformation monitoring. *Procedia Earth Planet. Sci.* 1(1): 1081-1088.

Kampes, B.M., 2005. *Displacement parameter estimation using permanent scatterer interferometry*. Delf Technical University, The Netherlands.

Li, Z., Muller, J.-P., Cross, P., Fielding, E.J., 2005. Interferometric synthetic aperture radar (InSAR) atmospheric correction: GPS, Moderate Resolution Imaging Spectroradiometer (MODIS), and InSAR integration. *J. Geophys. Res. - Solid Earth* 110(B3), paper No. B03410.

Lyu, M., Ke, Y., Li, X., Zhu, L., Guo, L., Gong, H., 2020. Detection of seasonal deformation of highway overpasses using the PS-InSAR technique: A case study in Beijing urban area. *Remote Sens.* 12(18), paper No. 3071.

Macchiarulo, V., Milillo, P., De Jong, M.J., González Martí, J., Sánchez, J., Giardina, G.J.S.C., Monitoring, H., 2021. Integrated InSAR monitoring and structural assessment of tunnelling-induced building deformations 28(9), paper No. e2781.

Miranda, N., Rosich, B., Santella, C., Grion, M., 2005. Review of the Impact of ERS-2 Piloting Modes on the SAR Doppler Stability. In: Proc. 2004 Envisat & ERS Symposium, 6-10 September 2004, Salzburg, Austria.

Mirzadeh, S.M.J., Jin, S., Parizi, E., Chaussard, E., Bürgmann, R., Delgado Blasco, J.M., Amani, M., Bao, H., Mirzadeh, S.H., 2021. Characterization of Irreversible Land Subsidence in the Yazd-Ardakan Plain, Iran From 2003 to 2020 InSAR Time Series. *J. Geophys. Res. - Solid Earth* 126(11), paper Id e2021JB022258.

Modeste, G., Doubre, C.,Masson, F., 2021. Time evolution of mining-related residual subsidence monitored over a 24-year period using InSAR in southern Alsace, France. *Int. J. Appl. Earth Obs. Geoinform.* 102, paper No. 102392.

Mohamadi, B., Balz, T., Younes, A., 2019. A Model for Complex Subsidence Causality Interpretation Based on PS-InSAR Cross-Heading Orbits Analysis. *Remote Sens.* 11(17), 2014.

Nappo, N., Ferrario, M.F., Livio, F., Michetti, A.M., 2020. Regression Analysis of Subsidence in the Como Basin (Northern Italy): New Insights on Natural and Anthropic Drivers from InSAR Data. *Remote Sens.* 12(18), 2931.

Nappo, N., Peduto, D., Polcari, M., Livio, F., Ferrario, M.F., Comerci, V., Stramondo, S., Michetti, A.M., 2021. Subsidence in Como historic centre (northern Italy): Assessment of building vulnerability combining hydrogeological and stratigraphic features, Cosmo-SkyMed InSAR and damage data. *Int. J. Disaster Risk Reduct.* 56, paper No. 102115.

Nilfouroushan, F., Gido, N.A.A., Darvishi, M., 2022. Cross-checking of the nationwide Ground Motion Service (GMS) of Sweden with the previous InSAR-based results: Case studies of Uppsala and Gävle Cities. EGU General Assembly 2022, Vienna, Austria, 23–27 May 2022, paper No. EGU22-5293

Peng, M., Lu, Z., Zhao, C., Motagh, M., Bai, L., Conway, B.D., Chen, H., 2022. Mapping land subsidence and aquifer system properties of the Willcox Basin, Arizona, from InSAR observations and independent component analysis. *Remote Sens. Env.* 271, paper No. 112894.

Perissin, D., Wang, Z., Wang, T., 2011: The SARPROZ InSAR tool for urban subsidence/manmade structure stability monitoring in China. In: Proc. ISRSE, Sydney.

Psimoulis, P., Ghilardi, M., Fouache, E.,Stiros, S., 2007. Subsidence and evolution of the Thessaloniki plain, Greece, based on historical leveling and GPS data. *Eng. Geol.* 90(1): 55-70.

Regione Lombardia, 2022. Carta Tecnica Regionale. Collezione di dati territoriali, Regione Lombardia. Available online at geoportale.regione.lombardia.it/download-ctr (last access on 25th September 2022).

Regione Lombardia, 2018. Carta Geologica 250.000. Collezione di dati territoriali geoportale. Available online at regione.lombardia.it (last access on 25th September 2022).

Ruiz-Armenteros, A.M., Delgado, J.M., Bakon, M., Sousa, J.J., Lamas-Fernández, F., Marchamalo-Sacristán, M., Sánchez-Ballesteros, V., Papco, J., González-Rodrigo, B., Lazecky, M., 2021: ReMoDams: Monitoring Dams from Space Using Satellite Radar Interferometry. In: Proc. IEEE Int. Geoscience and Remote Sensing Symp. (IGARSS) 2021, 5331-5334.

Shen, Z.K., Liu, Z., 2020. Integration of GPS and InSAR data for resolving 3-dimensional crustal deformation. *Earth Space Sci.* 7(4), 1036.

Shi, X., Chen, C., Dai, K., Deng, J., Wen, N., Yin, Y., Dong, X., 2022. Monitoring and Predicting the Subsidence of Dalian Jinzhou Bay International Airport, China by Integrating InSAR Observation and Terzaghi Consolidation Theory. *Remote Sens.* 14(10), 2332.

Solari, L., Del Soldato, M., Bianchini, S., Ciampalini, A., Ezquerro, P., Montalti, R., Raspini, F.,Moretti, S., 2018. From ERS 1/2 to Sentinel-1: Subsidence Monitoring in Italy in the Last Two Decades. *Front. Earth Sci.* 6, 149.

Tomás, R., Romero, R., Mulas, J., Marturià, J.J. et al., 2014. Radar interferometry techniques for the study of ground subsidence phenomena: a review of practical issues through cases in Spain. *Environ. Earth Sci.* 71(1), 163-181.

Trahan, D.B., 1982. Monitoring Local Subsidence in Areas of Potential Geopressured Fluid Withdrawal, Southwestern Louisiana. *Gulf Coast Ass. Geol. Soc. Trans.* 32, 231-236.

Ustun, A., Tusat, E., Yalvac, S., 2010: Preliminary results of land subsidence monitoring project in Konya Closed Basin between 2006–2009 by means of GNSS observations. *Nat. Hazards Earth Syst. Sci.* 10(6), 1151-1157.

Werner, C.L., Wegmüller, U., Strozzi, T., Wiesmann, A., 2003: Interferometric point target analysis for deformation mapping. IGARSS 2003. 2003 IEEE International Geoscience and Remote Sensing Symposium. Proceedings (IEEE Cat. No.03CH37477) 7, 4362-4364.

Wu, J.-C., Shi, X.-Q., Ye, S.-J., Xue, Y.-Q., Zhang, Y., Yu, J., 2009. Numerical simulation of land subsidence induced by groundwater overexploitation in Su-Xi-Chang area, China. *Environ. Geol.* 57(6), 1409-1421.

Xu, X., Sandwell, D.T., Klein, E., Bock, Y., 2021. Integrated Sentinel-1 InSAR and GNSS Time-Series Along the San Andreas Fault System. *J. Geophys. Res. - Solid Earth* 126(11), paper No. 22579.

Yan, Y., Yang, Q., Jia, Z., Zhang, X., Dai, H., Ng, A.H.-M., 2021. Integration of Multiband InSAR and Leveling Measurements for Analyzing the Surface Subsidence of Shield Tunneling at Beijing-Zhangzhou High-Speed Railway. *J. Sensors* 2021, paper No. 6640077.

Yang, X., Wang, D., Xu, Y., Hou, M., Wang, Z., 2022. Performance Assessment of InSAR-Based Vertical Displacement Monitoring of Sluices in Coastal Soft Soil Area. *ASCE J. Civil Eng.* 26(1), 371-380.